

Keywords

Functionally Graded Anisotropic Structure, Dual Reciprocity Boundary Element Method, Design Sensitivity Analysis, Magneto-Thermoelasticity, Initial Stress

Received: July 12, 2017

Accepted: October 16, 2017

Published: November 9, 2017

Implicit Time-Stepping DRBEM for Design Sensitivity Analysis of Magneto-Thermo- Elastic FGA Structure Under Initial Stress

Mohamed Abdelsabour Fahmy^{1,2,*}, Saleh Manea Al-Harbi¹,
Badr Hamedy Al-Harbi¹

¹Mathematics Department, Jamoum University College, Umm Al-Qura University, Makkah, Saudi Arabia

²Basic Sciences Department, Faculty of Computers and Informatics, Suez Canal University, Ismailia, Egypt

Email address

maselim@uqu.edu.sa (M. A. Fahmy), salharbi434@yahoo.com (S. M. Al-Harbi),
bhharbi@uqu.edu.sa (B. H. Al-Harbi)

*Corresponding author

Citation

Mohamed Abdelsabour Fahmy, Saleh Manea Al-Harbi, Badr Hamedy Al-Harbi. Implicit Time-Stepping DRBEM for Design Sensitivity Analysis of Magneto-Thermo- Elastic FGA Structure Under Initial Stress. *American Journal of Mathematical and Computational Sciences*. Vol. 2, No. 6, 2017, pp. 55-62.

Abstract

The main objective of this paper is to evaluate the effects of functionally graded, rotation and initial stress on the displacement design sensitivities of the magneto-thermo-elastic functionally graded anisotropic (FGA) structures subjected to moving heat source. An implicit time-stepping scheme based on the dual reciprocity boundary element method (DRBEM) was used to obtain the temperature and displacement components. Also, an implicit differentiation of the discretized boundary integral equation with respect to design variables is used to calculate displacement design sensitivities of FGA structures with very high accuracy. The validity of the proposed method is examined and excellent agreement is obtained with existent results. The numerical results show our method is strong and efficient.

1. Introduction

The dynamical interaction between the thermal and mechanical fields in anisotropic materials has great practical applications in modern aeronautics, astronautics, nuclear reactors, earthquake engineering and high-energy particle accelerators. In recent years, an important number of engineering and mathematical papers devoted to the numerical solution have studied the overall behavior of such materials [1-11].

The development of initial stresses in the medium can be associated with many reasons, for example: difference of temperature, process of quenching, shot pinning and cold working, slow process of creep, differential external forces, gravity variations, etc. Biot [12] studied the influence of these stresses on the propagation of stress waves. Fahmy [13, 14] used boundary element method to obtain thermal stresses in a non-homogeneous anisotropic solid. The dual reciprocity boundary element method (DRBEM) was introduced by Nardini and Brebbia [15] for elastodynamic problems and extended to time-domain problems by Wrobel [16]. A more extensive historical review and applications of DRBEM may be found in Refs. [17-41].

The main aim of this paper is to study the influence of functionally graded, rotation and initial stress on the displacement design sensitivities of the magneto-thermo-elastic FGA structures subjected to moving heat source. The governing equations are solved using DRBEM and the numerical calculations are carried out for the temperature and displacement components. Then, an implicit differentiation method was used to compute the temperature design sensitivity and displacement design sensitivity with respect to design variables with very high accuracy. The obtained numerical results are compared with existent results to demonstrate the validity of the proposed method. The numerical results show our method is efficient and precise.

2. Formulation of the Problem

With reference to a Cartesian frame denoted by $Oxyz$, consider initially stressed thermoelastic FGA structure subjected to moving heat source and placed in a constant primary magnetic field H_0 acting in the direction of the z -axis and rotating about this axis. Here we address the generalized two-dimensional deformation problem as shown in Figure 1.

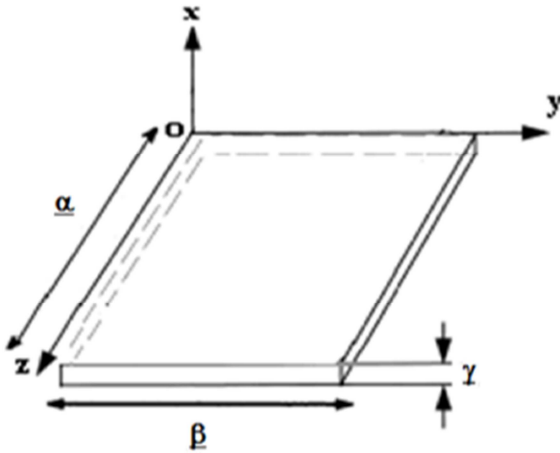


Figure 1. The coordinate system of the structure.

The governing equations of magneto-thermo-elasticity for an anisotropic solid in the presence of moving heat-source can be written as follows [42]

$$\sigma_{pj,j} + \tau_{pj,j} - \Gamma_{pj} - \rho(x+1)^m \omega^2 x_p = \rho(x+1)^m \ddot{u}_p \quad (1)$$

$$\sigma_{pj} = (x+1)^m \left(C_{pjkl} u_{k,l} - \beta_{pj} T(x,y,\tau) \right), C_{pjkl} = C_{klpj} = C_{jpk l}, \beta_{pj} = \beta_{jp} \quad (2)$$

$$\tau_{pj} = \mu(x+1)^m (h_p H_j + h_j H_p - \delta_{jp} (h_k H_k)), h_p = (\nabla \times (\mathbf{u} \times \mathbf{H}))_p \quad (3)$$

$$\Gamma_{pj} = P(x+1)^m \left(\frac{\partial u_j}{\partial x_p} - \frac{\partial u_p}{\partial x_j} \right) \quad (4)$$

$$k_{pj} T_{,pj} = c \rho \dot{T} - \rho \dot{\mathfrak{X}} k_{pj} = k_{jp}, (k_{12})^2 - k_{11} k_{22} < 0 \quad (5)$$

With the heat flux vector q_p given by Fourier's law

$$q_p = -k_{pj} T_{,j} \quad (6)$$

where σ_{pj} is the mechanical stress tensor, τ_{pj} Maxwell's electromagnetic stress tensor, u_k is the displacement, T is the temperature, P is the initial stress, C_{pjkl} and β_{pj} are respectively, the constant elastic moduli and stress-temperature coefficients of the anisotropic medium, μ is the magnetic permeability, h is the perturbed magnetic field, ω is the uniform angular velocity, k_{pj} are the thermal conductivity coefficients, ρ is the density, m is functionally graded parameter, c is the specific heat capacity of the solid, τ is the time and \mathfrak{X} is the moving heat source. Also, Ψ_k , δ_k , \bar{H} and \bar{h} are suitably prescribed functions and t_k are the tractions defined by $t_k = \sigma_{kj} n_j$.

The initial and boundary conditions for the current problem are assumed to be written as

$$u_k(x,y,0) = \dot{u}_k(x,y,0) = 0 \text{ for } (x,y) \in R \cup C \quad (7)$$

$$u_k(x,y,\tau) = \Psi_k(x,y,\tau) \text{ for } (x,y) \in C_3 \quad (8)$$

$$t_k(x,y,\tau) = \delta_k(x,y,\tau) \text{ for } (x,y) \in C_4, \tau > 0, C = C_3 \cup C_4, C_3 \cap C_4 = \emptyset \quad (9)$$

$$T(x,y,0) = f(x,y) \text{ for } (x,y) \in R \cup C \quad (10)$$

$$T(x,y,\tau) = \bar{H}(x,y,\tau) \text{ for } (x,y) \in C_1, \tau > 0 \quad (11)$$

$$q(x,y,\tau) = \bar{h}(x,y,\tau) \text{ for } (x,y) \in C_2, \tau > 0, C = C_1 \cup C_2, C_1 \cap C_2 = \emptyset \quad (12)$$

A superposed dot denotes differentiation with respect to the time and a comma followed by a subscript denotes partial differentiation with respect to the corresponding coordinates.

3. Numerical Scheme

The main objective of the numerical scheme is to describe the implementation of the DRBEM formulation for the solution of the Eqs. (1) and (5).

3.1. Temperature Field

From Eq. (5) using the DRBEM as described in Ref. 43, we obtain the representation formula

$$T(\xi) = \int_C (q^* T - T^* q) dC - \int_R (c \rho \dot{T} - \rho \dot{\mathfrak{X}}) T^* dR \quad (13)$$

To transform the domain integral in (13) to the boundary, the generalized source term is approximated with a series of given source terms f^q and unknown coefficients $\bar{\alpha}^q$ as follows

$$\int_R (c \rho \dot{T} - \rho \dot{\mathfrak{X}}) T^* dR \approx \sum_{q=1}^N \bar{\alpha}^q \int_R f^q T^* dR \quad (14)$$

Consequently, the dual reciprocity representation formula can be written as follows

$$T(\xi) + \int_C (T^* q - q^* T) dC = \sum_{q=1}^N \left(T^q(\xi) + \int_C (T^* q^q - q^* T^q) dC \right) \bar{\alpha}^q \quad (15)$$

The field variables T and q and the particular solutions T^q and q^q are then approximated as

$$\{T, q\} \approx \sum_{k=1}^N \bar{\varphi}_k \{\check{T}_k, \check{q}_k\} = \bar{\Phi}^T \{\check{T}, \check{q}\}, \{T^q, q^q\} \approx \sum_{k=1}^N \bar{\varphi}_k \{\check{T}_k^q, \check{q}_k^q\} = \bar{\Phi}^T \{\check{T}^q, \check{q}^q\} \quad (16)$$

where $\check{T}, \check{q}, \check{T}^q, \check{q}^q$ and $\bar{\Phi}$ are matrices

Using (16) and applying the point collocation procedure to (15), we have the following system

$$\bar{\zeta} \check{T} - \bar{\eta} \check{q} = \sum_{q=1}^N (\bar{\zeta} \check{T}^q - \bar{\eta} \check{q}^q) \bar{\alpha}^q \quad (17)$$

Let

$$\check{T} = [\check{T}^1 \check{T}^2 \dots \check{T}^N], \bar{\varphi} = [\check{q}^1 \check{q}^2 \dots \check{q}^N], \bar{\alpha} = [\bar{\alpha}^1 \bar{\alpha}^2 \dots \bar{\alpha}^N]^T \quad (18)$$

Using (18) into (17) we have

$$\bar{\zeta} \check{T} - \bar{\eta} \check{q} = (\bar{\zeta} \check{T} - \bar{\eta} \bar{\varphi}) \bar{\alpha} \quad (19)$$

Where the matrices \check{T} and $\bar{\varphi}$ contain the particular

$$\begin{bmatrix} \bar{M}^{11} & \bar{M}^{12} \\ \bar{M}^{21} & \bar{M}^{22} \end{bmatrix} \begin{bmatrix} \check{T}^k(\tau) \\ \check{T}^u(\tau) \end{bmatrix} + \begin{bmatrix} \bar{\zeta}^{11} & \bar{\zeta}^{12} \\ \bar{\zeta}^{21} & \bar{\zeta}^{22} \end{bmatrix} \begin{bmatrix} \check{T}^k(\tau) \\ \check{T}^u(\tau) \end{bmatrix} = \begin{bmatrix} \bar{\eta}^{11} & \bar{\eta}^{12} \\ \bar{\eta}^{21} & \bar{\eta}^{22} \end{bmatrix} \begin{bmatrix} \check{q}^k(\tau) \\ \check{q}^u(\tau) \end{bmatrix} + \begin{bmatrix} \check{B}^1(\tau) \\ \check{B}^2(\tau) \end{bmatrix} \quad (25)$$

The unknown fluxes $\check{q}^u(t)$ are obtained from the first row of matrix equation (25) are expressed as

$$\check{q}^u(\tau) = (\bar{\eta}^{12})^{-1} \left[\bar{M}^{11} \check{T}^k(\tau) + \bar{M}^{12} \check{T}^u(\tau) + \bar{\zeta}^{11} \check{T}^k(\tau) + \bar{\zeta}^{12} \check{T}^u(\tau) - \bar{\eta}^{11} \check{q}^k(\tau) - \check{B}^1(\tau) \right] \quad (26)$$

Making use of Eq. (26), we can write the second row of matrix equation (25) as follows

$$\bar{M}^u \check{T}^u(\tau) + \bar{\zeta}^u \check{T}^u(\tau) = \bar{Q}^k(\tau) \quad (27)$$

where

$$\begin{aligned} \bar{Q}^k(\tau) &= \check{B}^k(\tau) + \bar{\eta}^k \check{q}^k(\tau) - \bar{M}^k \check{T}^k(\tau) - \bar{\zeta}^k \check{T}^k(\tau), \\ \bar{M}^u &= \bar{M}^{22} - \bar{\eta}^{22} (\bar{\eta}^{12})^{-1} \bar{M}^{12}, & \bar{\zeta}^u &= \bar{\zeta}^{22} - \bar{\eta}^{22} (\bar{\eta}^{12})^{-1} \bar{\zeta}^{12}, \\ \check{B}^k(\tau) &= \check{B}^2(\tau) - \bar{\eta}^{22} (\bar{\eta}^{12})^{-1} \check{B}^1(\tau), & \bar{\eta}^k &= \bar{\eta}^{21} - \bar{\eta}^{22} (\bar{\eta}^{12})^{-1} \bar{\eta}^{11}, \\ \bar{M}^k &= \bar{M}^{21} - \bar{\eta}^{22} (\bar{\eta}^{12})^{-1} \bar{M}^{11}, & \bar{\zeta}^k &= \bar{\zeta}^{21} - \bar{\eta}^{22} (\bar{\eta}^{12})^{-1} \bar{\zeta}^{11}. \end{aligned}$$

By using finite difference scheme as described by Ref. 44, Eq. (23) can be written as follows

$$\bar{\zeta}^u \check{T}_{n+1}^u = \bar{Q}_{n+1}^k \quad (28)$$

Where $\bar{Q}_{n+1}^k = \bar{Q}_{n+1}^k + \frac{\bar{M}^u}{\Delta\tau} \check{T}_n^u, \bar{\zeta}^u = \frac{\bar{M}^u}{\Delta\tau} + \bar{\zeta}^u$

Thus, with $T(x, y, t)$ determined, the remaining task is to solve (1) subject to (2)-(4).

3.2. Displacement Field

Making use of (2)-(4), we can write (1) as follows

$$L_{pk} u_k = \rho \ddot{u}_p - \left((D_{pk} + \Lambda D_{p1k}) u_k + D_p T - P \varepsilon_{jp} - \rho \omega^2 x_p \right) = \rho \ddot{u}_p - \rho b_p = \rho b'_p \quad (29)$$

where

$$L_{pk} = D_{pjk} \frac{\partial}{\partial x_j}, D_{pjk} = C_{pjkl} \frac{\partial}{\partial x_l}, D_{pk} = \mu H_0^2 \left(\frac{\partial}{\partial x_p} + \delta_{p1} \Lambda \right) \frac{\partial}{\partial x_k}, D_p = -\beta_{pj} \left(\frac{\partial}{\partial x_j} + \delta_{j1} \Lambda \right), \varepsilon_{jp} = \left(\frac{\partial u_j}{\partial x_p} - \frac{\partial u_p}{\partial x_j} \right), \Lambda = \frac{m}{x + \alpha}$$

solutions.

Then, by applying a point collocation procedure to Eq. (18) we obtain

$$c \rho \check{T} - \rho \check{r} = \bar{F} \bar{\alpha}(\tau) \quad (20)$$

From Eq. (20) the following expression can be derived

$$\bar{\alpha}(\tau) = \bar{F}^{-1} (c \rho \check{T} - \rho \check{r}) \quad (21)$$

Which can be substituted into (19) producing

$$\bar{M} \check{T}(\tau) + \bar{\zeta} \check{T}(\tau) = \bar{\eta} \check{q}(\tau) + \check{B}(\tau) \quad (22)$$

where

$$\bar{M} = c \rho v, \check{B} = \rho v \check{r}, v = -(\bar{\zeta} \check{T} - \bar{\eta} \bar{\varphi}) \bar{F}^{-1} \quad (23)$$

In order to solve the system (22), the nodal vectors are subdivided into known and unknown parts denoted by the superscripts k and u

$$\{\check{T}^k, \check{q}^u\} \in C_1, \{\check{T}^u, \check{q}^k\} \in C_2 \quad (24)$$

The following matrix equation is obtained from (22):

According to Ref. 24, the representation formula may be written as

$$u_m(\xi) = \int_C (u_{mp}^*(x, \xi)t_p(x) - t_{mp}^*(x, \xi)u_p(x))dC - \int_R u_{mp}^*(x, \xi)\rho b_p'(x)dR \quad (30)$$

Let

$$\rho b_p' = \rho \ddot{u}_p - ((D_{pk} + \Lambda D_{p1k})u_k + D_p T - P \varepsilon_{jp} - \rho \omega^2 x_p) \approx \sum_{q=1}^N f_{pn}^q \alpha_n^q = \sum_{q=1}^N (L_{ji} u_{kn}^q) \alpha_n^q \quad (31)$$

We proceed in a manner similar to that used in Ref. 45, in order to obtain the following dual reciprocity representation formula

$$u_m(\xi) = \int_C (u_{mp}^* t_p - t_{mp}^* u_p) dC + \sum_{q=1}^N (u_{mn}^q(\xi) - \int_C (u_{mp}^* t_{pn}^q - t_{mp}^* u_{pn}^q) dC) \alpha_n^q \quad (32)$$

The representation formula (32) is only valid if ξ lies inside the domain R. To obtain an expression that contains only boundary variables, the load point ξ has to be moved to the boundary. Therefore, the boundary is deformed by a small circular region with radius ε around the load point $\xi \in C$ as shown in Figure 1.

Following Ref. 45, the dual reciprocity boundary integral equation can be expressed as follows

$$c_{pj} u_p(\varepsilon) + p.v. \int_C u_p t_{mp}^* d\Gamma - \int_C u_{mp}^* t_p d\Gamma = \sum_{q=1}^N (c_{pj} u_{pn}^q(\varepsilon) + p.v. \int_C u_{pn}^q t_{mp}^* d\Gamma - \int_C u_{mp}^* t_{pn}^q d\Gamma) \alpha_n^q \quad (33)$$

where p.v. means the principal value of the integral.

The unknown field variables and the particular solutions are respectively approximated by means of nodal values $[\cdot]_k$ and shape functions φ_k

$$\{u, t\} \approx \sum_{k=1}^N \varphi_k \{\check{u}_k, \check{t}_k\} = \Phi^T \{\check{u}, \check{t}\}, \{u^q, t^q\} \approx \sum_{k=1}^N \varphi_k \{\check{u}_k^q, \check{t}_k^q\} = \Phi^T \{\check{u}^q, \check{t}^q\} \quad (34)$$

where $\check{u}, \check{t}, \check{u}^q, \check{t}^q$ and Φ are matrices.

On the basis of these approximations, and using the point collocation procedure, the dual reciprocity boundary integral equation (33) results to the following system of equations

$$\zeta \check{u} - \eta \check{t} = \sum_{q=1}^N (\zeta \check{u}^q - \eta \check{t}^q) \alpha^q(\tau) \quad (35)$$

By letting

$$\check{U} = [\check{u}^1 \check{u}^2 \dots \check{u}^N], \check{\varphi} = [\check{t}^1 \check{t}^2 \dots \check{t}^N], \alpha = [\alpha^1 \alpha^2 \dots \alpha^N]^T \quad (36)$$

We can write (35) as follows

$$\zeta \check{u}(\tau) - \eta \check{t}(\tau) = (\zeta \check{U} - \eta \check{\varphi}) \alpha(\tau) \quad (37)$$

The coefficient vector $\alpha(\tau)$ can be calculated by setting up a system of N equations from (31) using the point collocation procedure, which yields

$$\rho \check{u}(\tau) - \rho \check{b}(\tau) = F \alpha(\tau) \quad (38)$$

Now, from (38), we may derive

$$\alpha(\tau) = F^{-1}(\rho \check{u}(\tau) - \rho \check{b}(\tau)) \quad (39)$$

Substitution of (39) into (37) yields the system

$$\mathcal{M} \check{u} + \zeta \check{u} = \eta \check{t}(\tau) + \check{B}(\tau) \quad (40)$$

where

$$\check{U} = (\eta \check{\varphi} - \zeta \check{U}) F^{-1}, \mathcal{M} = \rho \check{U}, \check{B}(\tau) = \rho \check{U} \check{b}(\tau). \quad (41)$$

By subdividing the nodal vectors into known and unknown parts as follows

$$\{\check{u}^k, \check{t}^u\} \in C_3, \{\check{u}^u, \check{t}^k\} \in C_4 \quad (42)$$

where the superscripts k and u denote, respectively, the known and unknown parts

Hence we can write the system (40) in the following form

$$\begin{bmatrix} \mathcal{M}^{11} & \mathcal{M}^{12} \\ \mathcal{M}^{21} & \mathcal{M}^{22} \end{bmatrix} \begin{bmatrix} \check{u}^k(\tau) \\ \check{u}^u(\tau) \end{bmatrix} + \begin{bmatrix} \zeta^{11} & \zeta^{12} \\ \zeta^{21} & \zeta^{22} \end{bmatrix} \begin{bmatrix} \check{u}^k(\tau) \\ \check{u}^u(\tau) \end{bmatrix} = \begin{bmatrix} \eta^{11} & \eta^{12} \\ \eta^{21} & \eta^{22} \end{bmatrix} \begin{bmatrix} \check{t}^k(\tau) \\ \check{t}^u(\tau) \end{bmatrix} + \begin{bmatrix} \check{B}^1(\tau) \\ \check{B}^2(\tau) \end{bmatrix} \quad (43)$$

The unknown fluxes $\check{t}^u(\tau)$ can be obtained from the first row of (43) as follows

$$\check{t}^u(\tau) = (\eta^{12})^{-1} [\mathcal{M}^{11} \check{u}^k(\tau) + \mathcal{M}^{12} \check{u}^u(\tau) + \zeta^{11} \check{u}^k(\tau) + \zeta^{12} \check{u}^u(\tau) - \eta^{11} \check{t}^k(\tau) - \check{B}^1(\tau)] \quad (44)$$

With the aid of (44) into the second row of (43) we obtain

$$\mathcal{M}^u \check{u}^u(\tau) + \zeta^u \check{u}^u(\tau) = Q^k(\tau) \quad (45)$$

where

$$Q^k(\tau) = \check{B}^k(\tau) + \eta^k \check{t}^k(\tau) - \mathcal{M}^k \check{u}^k(\tau) - \zeta^k \check{u}^k(\tau), \check{B}^k(\tau) = \mathcal{B}^2(\tau) - \eta^{22} (\eta^{12})^{-1} \mathcal{B}^1(\tau),$$

$$\begin{aligned} \mathcal{M}^u &= \mathcal{M}^{22} - \eta^{22}(\eta^{12})^{-1}\mathcal{M}^{12}, & \zeta^u &= \zeta^{22} - \eta^{22}(\eta^{12})^{-1}\zeta^{12}, \\ \mathcal{M}^k &= \mathcal{M}^{21} - \eta^{22}(\eta^{12})^{-1}\mathcal{M}^{11}, & \zeta^k &= \zeta^{21} - \eta^{22}(\eta^{12})^{-1}\zeta^{11}. \end{aligned}$$

We can write (45) at time step $n + 1$

$$\mathcal{M}^u \check{u}_{n+1}^u(\tau) + \zeta^u \check{u}_{n+1}^u(\tau) = Q_{n+1}^k(\tau) \tag{46}$$

where

$$Q_{n+1}^k(\tau) = \check{B}_{n+1}^k(\tau) + \eta^k \check{t}_{n+1}^k(\tau) - \mathcal{M}^k \check{u}_{n+1}^k(\tau) - \zeta^k \check{u}_{n+1}^k(\tau)$$

Now, we consider an implicit backward finite difference scheme for solving the system of ordinary differential equations (46), the so-called Houbolt’s algorithm is applied to reduce (46) to an algebraic system. To do this, the velocities \dot{u}_{n+1} and accelerations \ddot{u}_{n+1} at time step $n + 1$ are approximated as [43]

$$\check{u}_{n+1} \approx \frac{1}{6\Delta t} (11\check{u}_{n+1} - 18\check{u}_n + 9\check{u}_{n-1} - 2\check{u}_{n-2}) \tag{47}$$

$$\check{\ddot{u}}_{n+1} \approx \frac{1}{\Delta t^2} (2\check{u}_{n+1} - 5\check{u}_n + 4\check{u}_{n-1} - \check{u}_{n-2}) \tag{48}$$

Substituting (47) and (48) into (46) we have

$$\zeta^u \check{u}_{n+1}^u(\tau) = Q_{n+1}^k(\tau) \tag{49}$$

Where $\zeta^u = \frac{2\mathcal{M}^u}{\Delta t^2} + \zeta^u$, $Q_{n+1}^k = Q_{n+1}^k + \frac{\mathcal{M}^u}{\Delta t^2} (5\check{u}_n - 4\check{u}_{n-1} + \check{u}_{n-2})$

Applying the same technique described in Ref. 38, we can obtain the unknown \check{u}_{n+1}^u , $\check{\ddot{u}}_{n+1}^u$ and t_{n+1}^u from (47), (48) and (44) respectively.

Thus, the displacement design sensitivity is performed by implicit differentiation of equation (49) and also the temperature design sensitivity is performed by implicit differentiation of equation (28).

$$k_{pj} = \begin{bmatrix} 5.2 & 0 & 0 \\ 0 & 7.6 & 0 \\ 0 & 0 & 38.3 \end{bmatrix} \text{ W/Km}$$

Mass density $\rho = 7820 \text{ Kg/m}^3$ and heat capacity $c = 461 \text{ J/Kg K}$, $H_0 = 1000000 \text{ Oersted}$, $\mu = 0.5 \text{ Gauss/Oersted}$, $\tau_0 = 0.5$, $m = 0.5$, $\Delta\tau = 0.0001$. The numerical values of the temperature and displacement are obtained by discretizing the boundary into 120 elements ($N_b = 120$) and choosing 60 well spaced out collocation points ($N_i = 60$) in the interior of the solution domain [44-46].

4. Numerical Results and Discussion

We assume that the moving heat source takes the following form

$$\mathfrak{X}(x, y, \tau) = \frac{Q_0 H(v\tau) \sinh(x)}{\sqrt{y^2 + v^2}}$$

Where H is the Heaviside unit step function, Q_0 is the heat source strength and v its velocity and all are constants.

In order to illustrate the theoretical results obtained in the preceding sections, the material chosen for this purpose is monoclinic graphite-epoxy with physical data given as

Elasticity tensor

$$C_{pjkl} = \begin{bmatrix} 430.1 & 130.4 & 18.2 & 0 & 0 & 201.3 \\ 130.4 & 116.7 & 21.0 & 0 & 0 & 70.1 \\ 18.2 & 21.0 & 73.6 & 0 & 0 & 2.4 \\ 0 & 0 & 0 & 19.8 & -8.0 & 0 \\ 0 & 0 & 0 & -8.0 & 29.1 & 0 \\ 201.3 & 70.1 & 2.4 & 0 & 0 & 147.3 \end{bmatrix} \text{ GPa}$$

Mechanical temperature coefficient

$$\beta_{pj} = \begin{bmatrix} 1.01 & 2.00 & 0 \\ 2.00 & 1.48 & 0 \\ 0 & 0 & 7.52 \end{bmatrix} \cdot 10^6 \text{ N/Km}^2$$

Tensor of thermal conductivity

The initial and boundary conditions considered in the calculations are

$$\text{at } \tau = 0 \quad \dot{u}_1 = \dot{u}_2 = \ddot{u}_1 = \ddot{u}_2, \dot{T} = 0$$

$$\text{at } x = 0 \quad \frac{\partial u_1}{\partial x} = \frac{\partial u_2}{\partial x} = 0, \frac{\partial T}{\partial x} = 0$$

$$\text{at } x = 1 \quad \frac{\partial u_1}{\partial x} = \frac{\partial u_2}{\partial x} = 0, \frac{\partial T}{\partial x} = 0$$

$$\text{at } y = 0 \quad \frac{\partial u_1}{\partial y} = \frac{\partial u_2}{\partial y} = 0, \frac{\partial T}{\partial y} = 0$$

$$\text{at } y = 1 \quad \frac{\partial u_1}{\partial y} = \frac{\partial u_2}{\partial y} = 0, \frac{\partial T}{\partial y} = 0$$

In order to get the influence of the functionally graded, rotation and initial stress parameters on the displacement design sensitivities, we assume that the presence of each parameter takes the value 0.5 and the absence of each parameter takes the value 0 and the results presented graphically in Figures 2 and 3.

Figure 2. Shows the variation of the displacement u_1 sensitivity with the time under the effects of functionally graded, rotation and initial stress. The figure indicates that the displacement u_1 sensitivity records higher values in the case of presence of rotation parameter and absence of functionally graded and initial stress parameters.

Figure 3. Shows the variation of the displacement u_2 sensitivity with the time under the effects of functionally

graded, rotation and initial stress. The figure indicates that the displacement u_2 sensitivity records higher values in the case of presence of functionally graded parameter and absence of rotation and initial stress parameters.

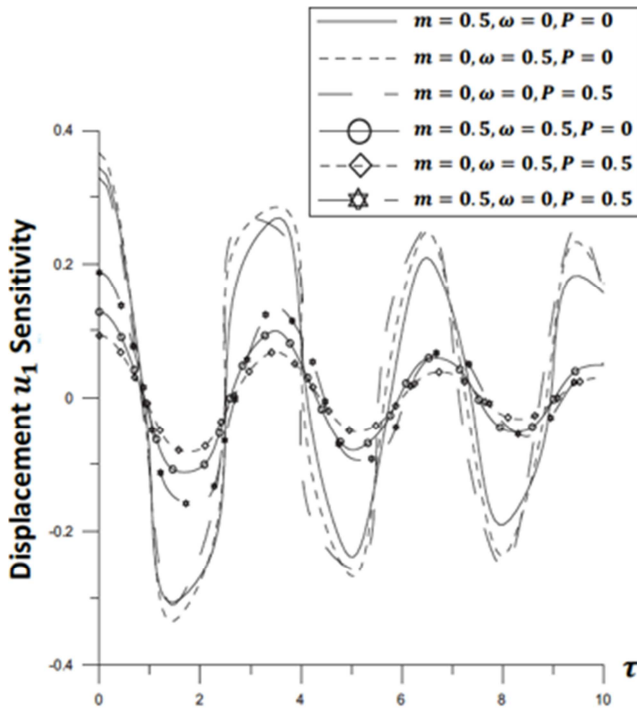


Figure 2. Variation of the displacement u_1 sensitivity with time τ .

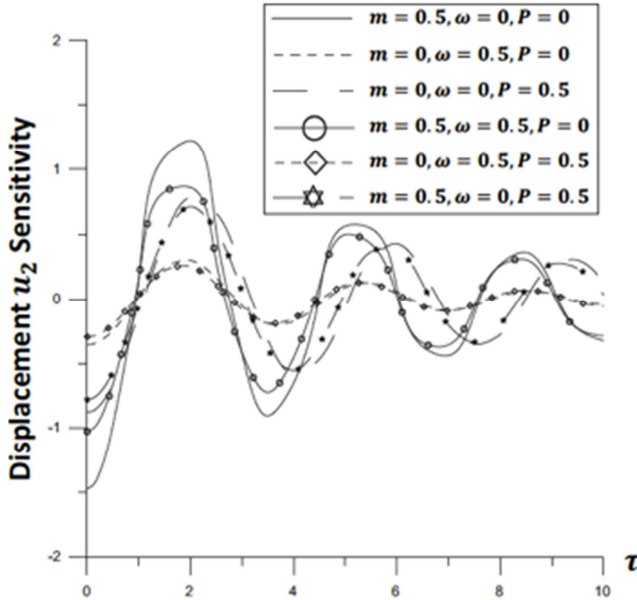


Figure 3. Variation of the displacement u_2 sensitivity with time τ .

The present work should be applicable to any design sensitivity of magneto-thermoelastic problem. The example considered by Sladek *et al.* [47] may be considered as a special case of the current general problem in the context of the uncoupled thermoelasticity theory. Also, there are a lot of practical applications may be deduced as special cases from this general study and may be implemented in commercial

finite element method (FEM) software packages FlexPDE 6. In the special case under consideration, the numerical results of the temperature with the time are plotted in Figure 4 to show the validity of the DRBEM. The obtained DRBEM results have been compared graphically with the obtained Meshless Local Petrov–Galerkin (MLPG) method results of Sladek *et al.* [47] and also the obtained FlexPDE 6 results are shown graphically in the same figure to confirm the validity of the proposed method. It can be seen from this figure that the DRBEM results are in excellent agreement with the results obtained by MLPG and FEM, thus confirming the accuracy of the DRBEM.

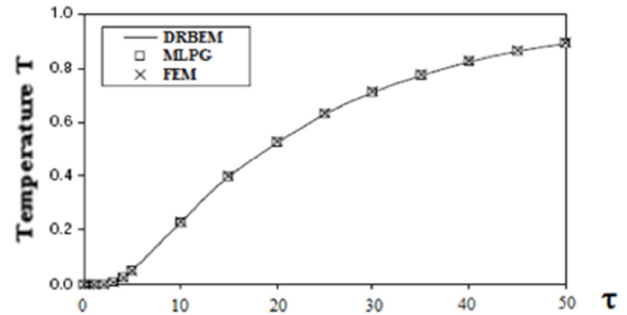


Figure 2. Variation of the temperature T with time τ for three methods: DRBEM, MLPG, FEM.

This phenomenon gives clear evidence of magneto-thermo-elastic effect in initially stressed FGA structure rotating about its axis and subjected to moving heat source. From this knowledge of transient variations of displacement components, we can design various initially stressed magneto thermoelastic structures under rotation load to meet specific engineering requirements and utilize it in measurement techniques of magneto-thermo-elasticity.

5. Conclusion

The DRBEM is more efficient and easy to use than FEM because it only needs the boundary of the integration domain to be discretized into elements.

For closed or open boundary problem the users of need only to deal with real geometry boundaries. Most problems of design sensitivity analysis of magneto-thermo- elastic FGA structures are associated with open boundary structures. For these open boundary structures, the users of FEM use artificial boundaries, which are far away from the real structure. So, DRBEM becomes the best method for the general problem considered in this study.

From the present research that has been performed, it is possible to conclude that the design of the structure is sensitive to boundary shape. Also from this knowledge of the variation of the displacements and temperature sensitivities with time under the effects of functionally graded, rotation and initial stress on the magneto-thermo-elastic functionally graded anisotropic (FGA) structures subjected to moving heat source, we can design various structures to meet specific design requirements and put them to appropriate use, will be better able to design structures.

References

- [1] A. M. Abd-Alla, A. M. El-Naggar, and M. A. Fahmy, "Magneto-thermoelastic problem in non-homogeneous isotropic cylinder," *Heat Mass Transfer* 39, 625-629 (2003).
- [2] A. M. Abd-Alla, T. M. El-Shahat, and M. A. Fahmy, "Thermoelastic stresses in inhomogeneous anisotropic solid in the presence of body force," *Int. J. Heat Technol.* 25, 111-118 (2007).
- [3] A. M. Abd-Alla, M. A. Fahmy, and T. M. El-Shahat, "Magneto-thermo-elastic stresses in inhomogeneous anisotropic solid in the presence of body force," *Far East J. Appl. Math.* 27, 499-516 (2007).
- [4] A. M. El-Naggar, A. M. Abd-Alla, and M. A. Fahmy, and S. M. Ahmed, "thermal stresses in a rotating non-homogeneous orthotropic hollow cylinder," *Heat Mass Transfer* 39, 41-46 (2002).
- [5] A. M. El-Naggar, A. M. Abd-Alla, M. A. Fahmy, "The propagation of thermal stresses in an infinite elastic slab," *Appl. Math. Comput.* 157, 307-312 (2004).
- [6] M. A. Fahmy and T. M. El-Shahat, "The effect of initial stress and inhomogeneity on the thermoelastic stresses in a rotating anisotropic solid," *Arch. Appl. Mech.* 78, 431-442 (2008).
- [7] A. N. Abd-Alla, and F. A. Alsheikh, "Reflection and refraction of plane quasi-longitudinal waves at an interface of two piezoelectric media under initial stresses," *Arch. Appl. Mech.* 79, 843-857 (2009).
- [8] M. A. Fahmy, "Shape design sensitivity and optimization for two-temperature generalized magneto-thermoelastic problems using time-domain DRBEM," *J. Therm. Stresses* 41, 119-138 (2018).
- [9] P. Singh, I. Couckuyt, K. Elsayed, D. Deschrijver, and T. Dhaene, "Shape optimization of a cyclone separator using multi-objective surrogate-based optimization," *Appl. Math. Modell.* 40, 4248-4259 (2016).
- [10] Computerized boundary element solutions for thermoelastic problems: Applications to functionally graded anisotropic structures, edited by M. A. Fahmy (LAP Lambert Academic Publishing, Saarbrücken, Germany, 2017), Chaps. 2 and 3.
- [11] A. Montoya, and H. Millwater, "Sensitivity analysis in thermoelastic problems using the complex finite element method," *J. Therm. Stresses* 40, 302-321 (2017).
- [12] M. A. Biot, "Mechanics of incremental deformation," Wiley, New York 1966.
- [13] M. A. Fahmy, "Effect of initial stress and inhomogeneity on magneto-thermo-elastic stresses in a rotating anisotropic solid," *JP J. Heat Mass Transfer* 1, 93-112 (2007).
- [14] M. A. Fahmy, "Thermoelastic stresses in a rotating non-homogeneous anisotropic body," *Numer. Heat Transfer, Part A*, 53, 1001-1011 (2008).
- [15] A new approach to free vibration analysis using boundary elements, edited by D. Nardini and C. A. Brebbia (Springer, Berlin, 1982), Chaps. 1 and 2.
- [16] The dual reciprocity boundary element formulation for transient heat conduction, edited by L. C. Wrobel, C. A. Brebbia, and D. Nardini (Springer, Berlin, 1986), Chaps. 2 and 3.
- [17] P. W. Partridge and L. C. Wrobel, "The dual reciprocity boundary element method for spontaneous ignition," *Int. J. Numer. Methods Eng.* 30, 953-963 (1990).
- [18] The dual reciprocity boundary element method, edited by P. W. Partridge, C. A. Brebbia, and L. C. Wrobel (Computational Mechanics Publications, Southampton, 1992), Chap. 2.
- [19] T. T. Yamada and L. C. Wrobel, "A new approach to magnetic field analysis by the dual reciprocity boundary element method," *Int. J. Numer. Methods Eng.* 36, 2073-2085 (1993).
- [20] Boundary element methods for engineers and scientists, edited by L. Gaul, M. Kögl, and M. Wagner (Springer-Verlag, Berlin 2003), Chap. 10.
- [21] B. I. Yun and W. T. Ang, "A dual-reciprocity boundary element approach for axisymmetric nonlinear time-dependent heat conduction in a non-homogeneous solid," *Eng. Anal. Boundary Elem.* 34, 697-706 (2010).
- [22] M. A. Fahmy Application of DRBEM to non-steady state heat conduction in non-homogeneous anisotropic media under various boundary elements. *Far East J. Math. Sci.* 43, 83-93 (2010).
- [23] M. A. Fahmy, "Transient magneto-thermoviscoelastic plane waves in a non-homogeneous anisotropic thick strip subjected to a moving heat source," *Applied Mathematical Modelling*, 36, 4565-4578 (2012).
- [24] M. A. Fahmy, "Numerical modeling of transient magneto-thermo-viscoelastic waves in a rotating nonhomogeneous anisotropic solid under initial stress," *International Journal of Modeling, Simulation and Scientific Computing*, 3, 1250002 (1-24) (2012).
- [25] M. A. Fahmy, "The effect of rotation and inhomogeneity on the transient magneto-thermoviscoelastic stresses in an anisotropic solid," *ASME Journal of Applied Mechanics*, 79, 1015 (2012).
- [26] M. A. Fahmy, "Transient magneto-thermo-viscoelastic stresses in a rotating nonhomogeneous anisotropic solid with and without a moving heat source," *Journal of Engineering Physics and Thermophysics*, 85, 950-958 (2012).
- [27] M. A. Fahmy, "Transient magneto-thermo-elastic stresses in an anisotropic viscoelastic solid with and without moving heat source," *Numerical Heat Transfer, Part A: Applications*, 61, 547-564 (2012).
- [28] M. A. Fahmy, "Implicit-Explicit time integration DRBEM for generalized magneto-thermoelasticity problems of rotating anisotropic viscoelastic functionally graded solids," *Engineering Analysis with Boundary Elements*, 37, 107-115 (2013).
- [29] M. A. Fahmy, "Generalized magneto-thermo-viscoelastic problems of rotating functionally graded anisotropic plates by the dual reciprocity boundary element method," *Journal of Thermal Stresses*, 36, 1-20 (2013).
- [30] M. A. Fahmy, "A three-dimensional generalized magneto-thermo-viscoelastic problem of a rotating functionally graded anisotropic solids with and without energy dissipation," *Numerical Heat Transfer, Part A: Applications*, 63, 713-733 (2013).
- [31] M. A. Fahmy, "A 2-D DRBEM for generalized magneto-thermo-viscoelastic transient response of rotating functionally graded anisotropic thick strip," *International Journal of Engineering and Technology Innovation*, 3, 70-85 (2013).

- [32] M. A. Fahmy, "The DRBEM solution of the generalized magneto-thermo-viscoelastic problems in 3D anisotropic functionally graded solids," I. Idelsohn, M. Papadrakakis, B. Schrefler (eds.), 5th International conference on coupled problems in science and engineering (Coupled Problems 2013), Ibiza, Spain, June 17-19, pp. 862-872 (2013).
- [33] M. A. Fahmy, A. M. Salem, M. S. Metwally and M. M. Rashid, "Computer Implementation of the DRBEM for Studying the Generalized Thermoelastic Responses of Functionally Graded Anisotropic Rotating Plates with One Relaxation Time," *International Journal of Applied Science and Technology*, 3, 130-140 (2013).
- [34] M. A. Fahmy, A. M. Salem, M. S. Metwally and M. M. Rashid, "Computer Implementation of the DRBEM for Studying the Classical Uncoupled Theory of Thermoelasticity of Functionally Graded Anisotropic Rotating Plates," *International Journal of Engineering Research and Applications*, 3, 1146-1154 (2013).
- [35] M. A. Fahmy, "A Computerized DRBEM model for generalized magneto-thermo-visco-elastic stress waves in functionally graded anisotropic thin film/substrate structures," *Latin American Journal of Solids and Structures*, 11, 386-409 (2014).
- [36] M. A. Fahmy (2014), A. M. Salem, M. S. Metwally and M. M. Rashid, "Computer Implementation of the Drbem for Studying the Classical Coupled Thermoelastic Responses of Functionally Graded Anisotropic Plates," *Physical Science International Journal*, 4, 674-685 (2014).
- [37] M. A. Fahmy, A. M. Salem, M. S. Metwally and M. M. Rashid, "Computer Implementation of the DRBEM for Studying the Generalized Thermo Elastic Responses of Functionally Graded Anisotropic Rotating Plates with Two Relaxation Times," *British Journal of Mathematics & Computer Science*, 4, 1010-1026 (2014).
- [38] M. A. Fahmy, "A 2D time domain DRBEM computer model for magneto-thermoelastic coupled wave propagation problems," *International Journal of Engineering and Technology Innovation*, 4, 138-151 (2014).
- [39] M. A. Fahmy, "Boundary Element Solution of 2D Coupled Problem in Anisotropic Piezoelectric FGM Plates," *Proceedings of the, B. Schrefler, E. Oñate and M. Papadrakakis (eds.), 6th International Conference on Computational Methods for Coupled Problems in Science and Engineering (Coupled Problems 2015), Venice. Italy, May 18-20, pp. 382-391 (2015).*
- [40] M. A. Fahmy (2016), Numerical Modeling of Coupled Thermoelasticity with relaxation times in Rotating FGAPs Subjected to a Moving Heat Source, *Physical Science International Journal*, Vol. 9, Issue 4, pp. 1-13.
- [41] M. A. Fahmy, "3D DRBEM Modeling for Rotating initially stressed Anisotropic functionally graded piezoelectric Plates," 7th European Congress on Computational Methods in Applied Sciences and Engineering (ECCOMAS 2016) M. Papadrakakis, V. Papadopoulos, G. Stefanou, V. Plevris (eds.), Crete Island, Greece, June 5–10 (2016).
- [42] M. A. Fahmy, "A time-stepping DRBEM for Magneto-thermo-viscoelastic interactions in a rotating nonhomogeneous anisotropic solid," *Int. J. Appl. Mech.* 3, 1-24 (2011).
- [43] M. A. Fahmy, "A time-stepping DRBEM for the transient magneto-thermo-visco-elastic stresses in a rotating non-homogeneous anisotropic solid," *Eng. Anal. Boundary Elem.* 36, 335-345 (2012).
- [44] M. A. Fahmy, "Finite difference algorithm for transient magneto-thermo-elastic stresses in a non-homogeneous solid cylinder," *Int. J. Mater. Eng. Technol.* 3, 87-93 (2010).
- [45] M. A. Fahmy, "Influence of inhomogeneity and initial stress on the transient magneto-thermo-visco-elastic stress waves in an anisotropic solid," *World J. Mech.* 1, 256-265 (2011).
- [46] A. M. Abd-Alla, M. A. Fahmy, and T. M. El-Shahat, "Magneto-thermo-elastic problem of a rotating non-homogeneous anisotropic solid cylinder," *Arch. Appl. Mech.* 78, 135-148 (2008).
- [47] Sladek, V. Sladek, P. Solec, and Ch. Zhang, "Fracture analysis in continuously nonhomogeneous magneto-electro-elastic solids under a thermal load by the MLPG," *Int. J. Solids and Struct.* 47, 1381-1391 (2010).